

Hydrochlorination of Ruthenaphosphaalkenyls: Unexpectedly Facile Access to Alkylchlorohydrophosphane Complexes.

V.K. Greenacre, I.J. Day, and I. R. Crossley*

Department of Chemistry, University of Sussex, Falmer, Brighton, UK

Supplementary Information

Computational Details	S2
Table S1: Electronic energies of compounds 1 , 2a , 3 , 4a , 6 and intermediary A	S3
Table S2: Comparative electronic energies for HCl addition reactions.	S3
Figure S1: Charge distribution plot of compound 3	S4
Figure S2: Charge distribution plot of intermediary A	S5
Figure S3: ³¹ P NMR signatures for compound 4a	S6
Figure S4: ³¹ P NMR signatures for compound 4b	S6
Figure S5: ³¹ P NMR signatures for compound 4c	S7
Figure S6: ³¹ P NMR signatures for compound 4d	S7
Figure S7: ³¹ P NMR signatures for compound 4e	S8
Figure S8: ³¹ P NMR signatures for compounds 3 and 6	S8
Figure S9: ³¹ P- ¹ H HMBC plots for 4a-e .	S9
Figure S10: ¹ H, ¹³ C{ ¹ H} and ¹⁹ F-NMR spectra for compound 4d	S9
Figure S11: ¹ H, ¹³ C{ ¹ H} and ³¹ P{ ¹ H} NMR spectra for nBuMe ₂ SiCH ₂ PCl ₂	S11
Figure S12: ¹ H and ¹³ C{ ¹ H} NMR spectra for 2d	S12
Figure S13: ¹ H and ¹³ C{ ¹ H} NMR spectra for 2e	S13
Figure S14: ¹ H and ¹³ C{ ¹ H} NMR spectra for 4a	S14
Figure S15: ¹ H and ¹³ C{ ¹ H} NMR spectra for 4b	S15
Figure S16: ¹ H and ¹³ C{ ¹ H} NMR spectra for 4c	S16
Figure S17: ¹ H and ¹³ C{ ¹ H} NMR spectra for 4e	S17

Computational Details

Calculations were performed using Gaussian 09W, Revision C.01,³⁹ running on an Intel Core i5-2500 (quad, 3.3 GHz), equipped with 4 GB RAM; results were visualized using GaussView 5.0. Geometries were optimized with the hybrid density functional B3LYP, using the RECP basis set Lanl2dz for Ru and 6-31G** for all other atoms. Minima were characterized by frequency calculations at the same level of theory. Single point energy calculations were subsequently performed with the B3LYP functional, using Lanl2dz for Ru and the 6-311+G** basis set for all other atoms; NBO calculations were performed at the same level of theory.

The supplemental file RuPHCl.xyz contains the computed Cartesian coordinates of compounds **1**, **2a**, **3**, **4a**, **6** and proposed intermediary **A**. The file may be opened as a text file to read the coordinates, or opened directly by a molecular modelling program such as Mercury (version 3.3 or later, <http://www.ccdc.cam.ac.uk/pages/Home.aspx>) for visualization and analysis.

Table S1: Electronic energies of compounds **1**, **2a**, **3**, **4a**, **6** and intermediary **A** (defined as 'X'), and summated energies with one and two equivalents of HCl.

X	E(X)		E(X + HCl)		E(X + 2HCl)	
	/a.u.	/kcal mol⁻¹	/a.u.	/kcal mol⁻¹	/a.u.	/kcal mol⁻¹
HCl	-460.8338442	-289177.846				
1	-3278.596984	-2057352.394	-3739.430829	-2346530.239	-4200.264673	-2635708.085
2a	-3530.044816	-2215138.422	-3990.878660	-2504316.268	-4451.712504	-2793494.113
A	-3990.904856	-2504332.706	-4451.738700	-2793510.552		
3	-3739.457921	-2346547.240	-4200.291765	-2635725.085		
4a	-4451.791213	-2793543.504				
6	-4200.343814	-2635757.747				

Table S2: Comparative electronic energies (kcal mol⁻¹) and ΔE_{react} for additions of HCl to 'X'.

X + nHCl → Y	E(X + nHCl)	E(Y)	ΔE_{react}
	/kcal mol⁻¹	/kcal mol⁻¹	/kcal mol⁻¹
1 + HCl → 3	-2346530.239	-2346547.240	-17.001
2a + HCl → A	-2504316.268	-2504332.706	-16.438
A + HCl → 4a	-2793510.552	-2793543.504	-32.952
3 + HCl → 6	-2635725.085	-2635757.747	-32.661
2a + 2HCl → 4a	-2793494.113	-2793543.504	-49.390
1 + 2HCl → 6	-2635708.085	-2635757.747	-49.662

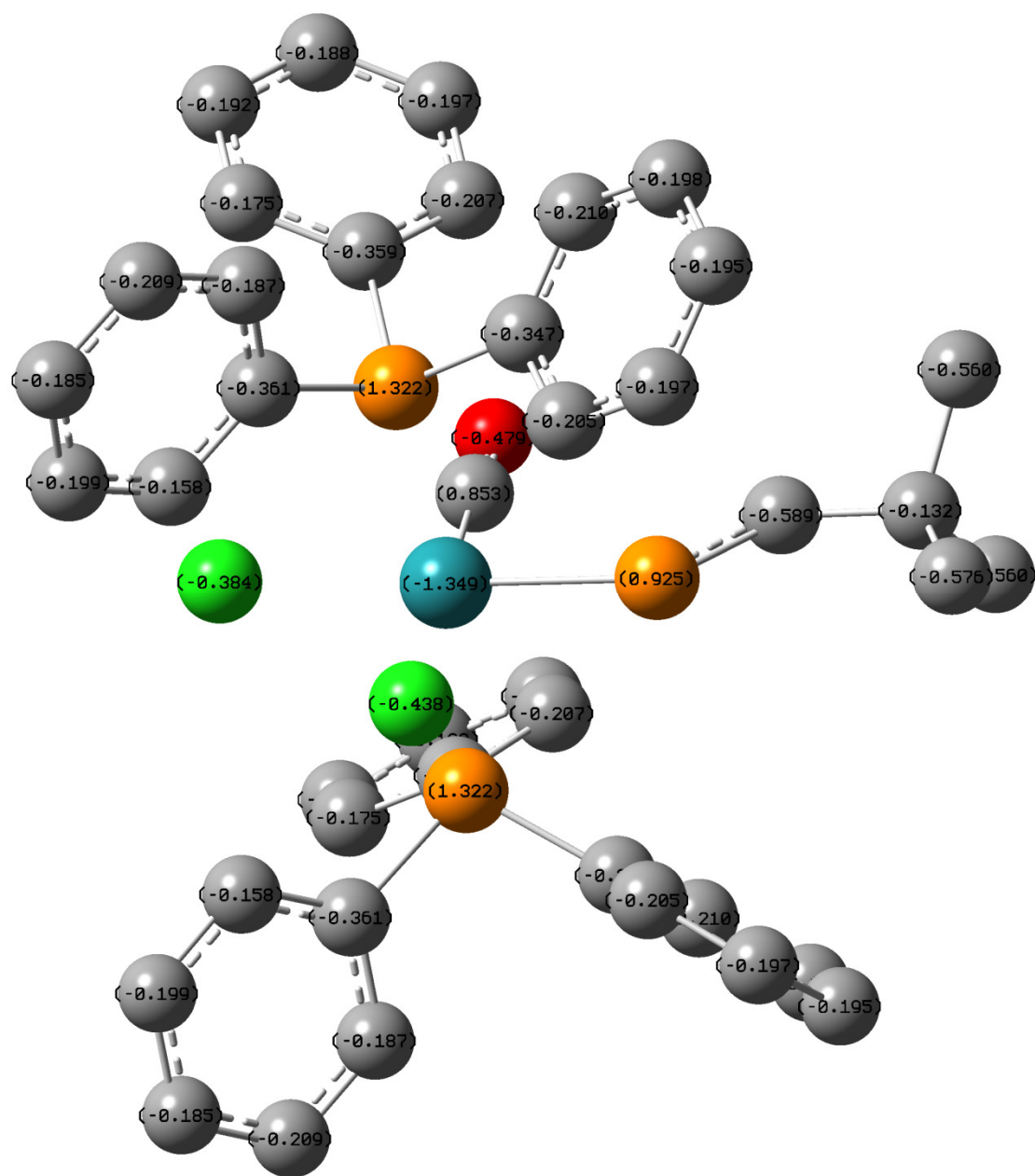


Figure S1: Distribution of NBO charge density for compound 3.

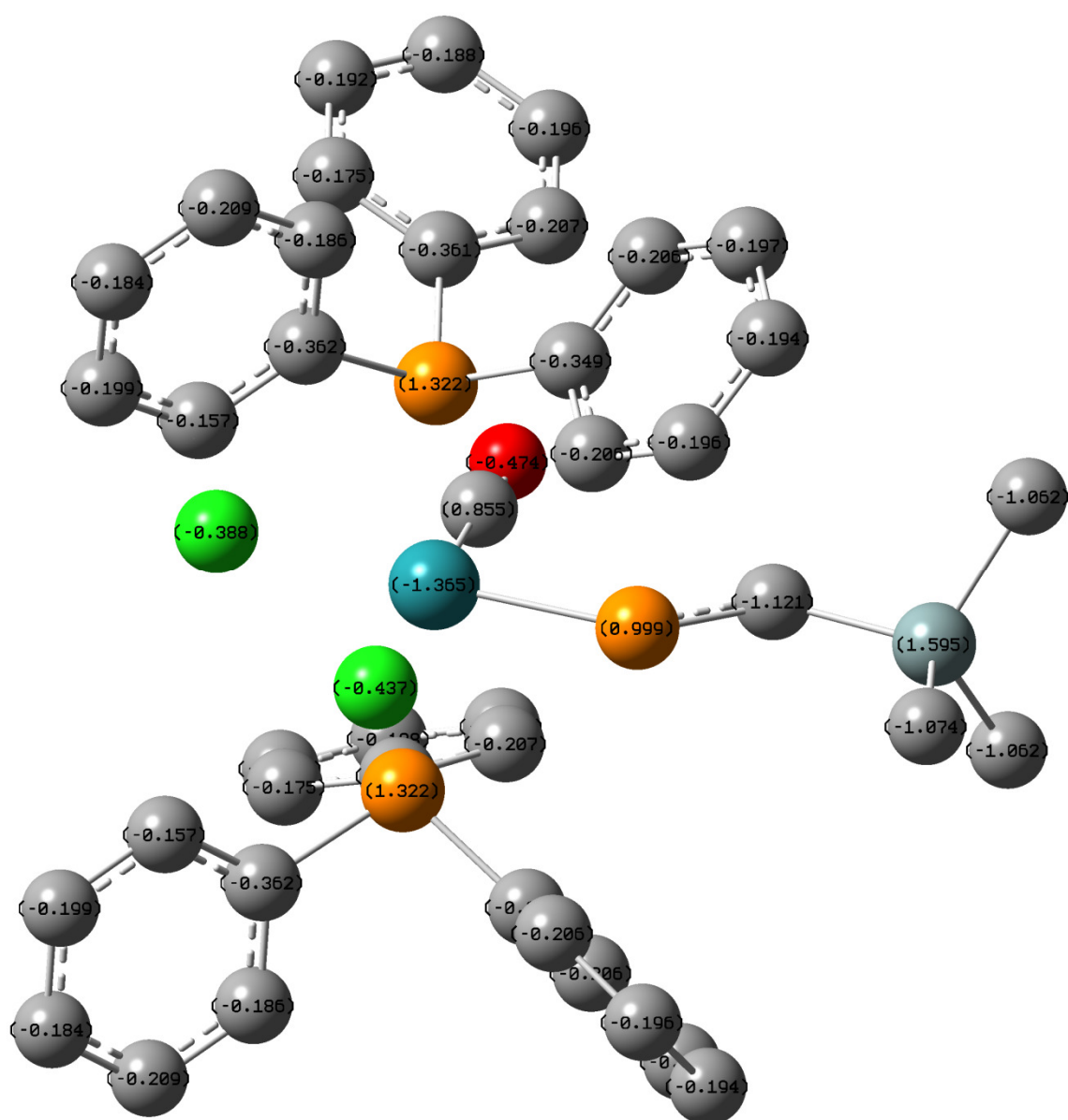


Figure S2: Distribution of NBO charge density for intermediary A.

Compound **4a**

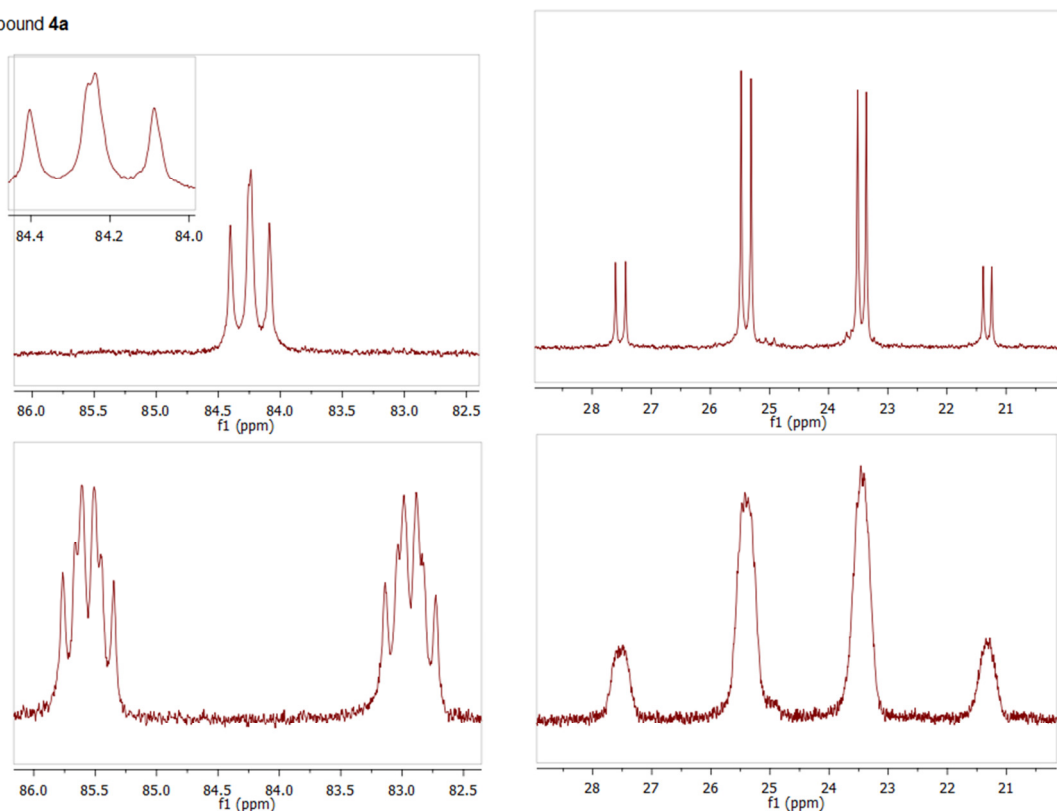


Figure S3. $^{31}\text{P}\{^1\text{H}\}$ (top) and ^{31}P (bottom) NMR signatures for $[\text{Ru}(\text{P}(\text{H})\text{ClCH}_2\text{SiMe}_3)\text{Cl}_2(\text{CO})(\text{PPh}_3)_2]$ (**4a**) plot on equivalent scales. The multiplicity of the chlorophosphane resonances is illustrated as inset for the proton decoupled spectrum.

Compound **4b**

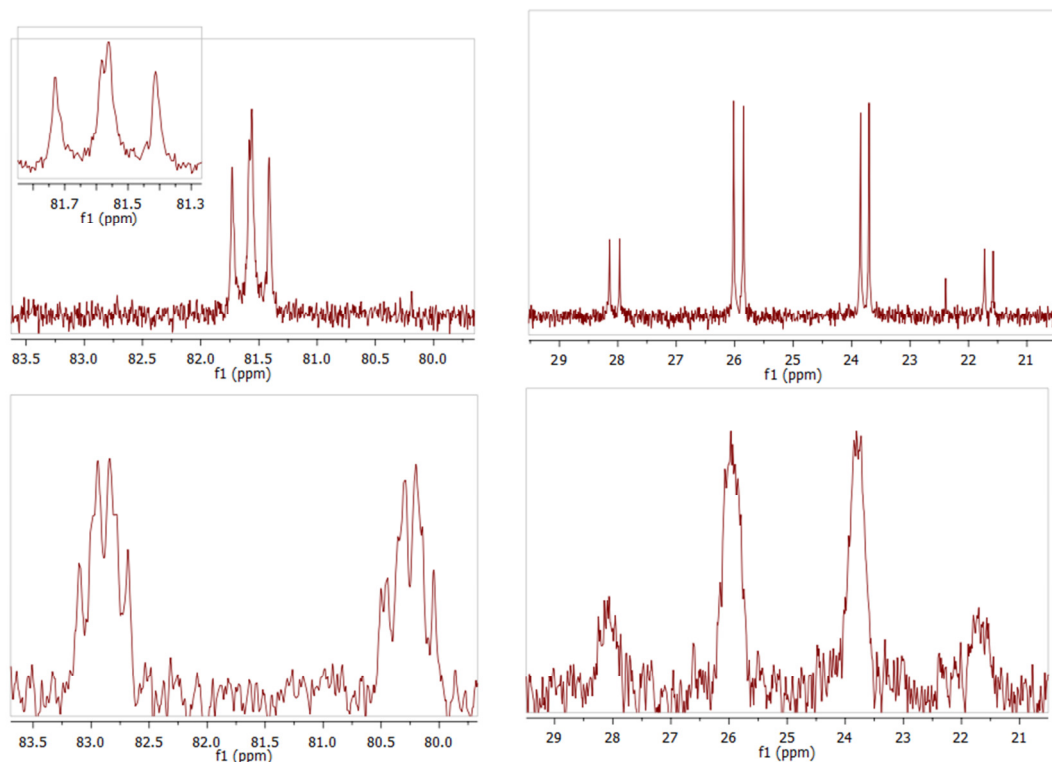


Figure S4. $^{31}\text{P}\{^1\text{H}\}$ (top) and ^{31}P (bottom) NMR signatures for $[\text{Ru}(\text{P}(\text{H})\text{ClCH}_2\text{SiMe}_2\text{Ph})\text{Cl}_2(\text{CO})(\text{PPh}_3)_2]$ (**4b**) plot on equivalent scales. The multiplicity of the chlorophosphane resonances is illustrated as inset for the proton decoupled spectrum.

Compound **4c**

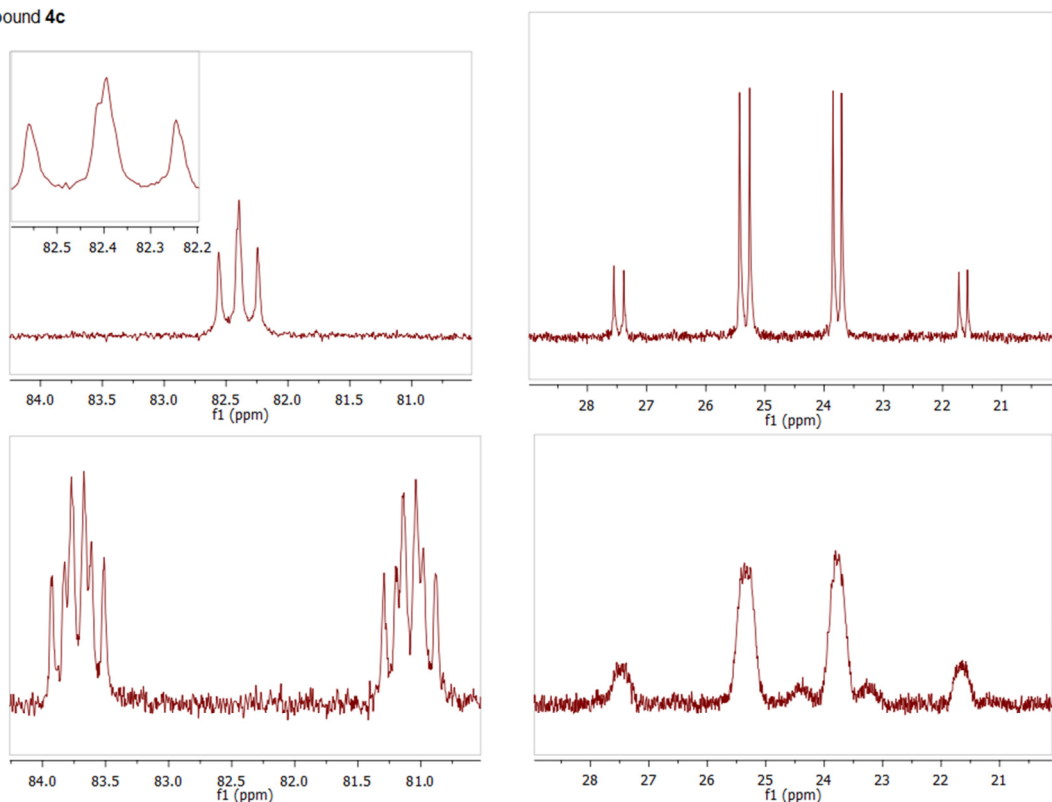


Figure S5. $^{31}\text{P}\{^1\text{H}\}$ (top) and ^{31}P (bottom) NMR signatures for $[\text{Ru}(\text{P}(\text{H})\text{ClCH}_2\text{SiMe}_2\text{Tol})\text{Cl}_2(\text{CO})(\text{PPh}_3)_2]$ (**4c**) plot on equivalent scales. The multiplicity of the chlorophosphane resonances is illustrated as inset for the proton decoupled spectrum.

Compound **4d**

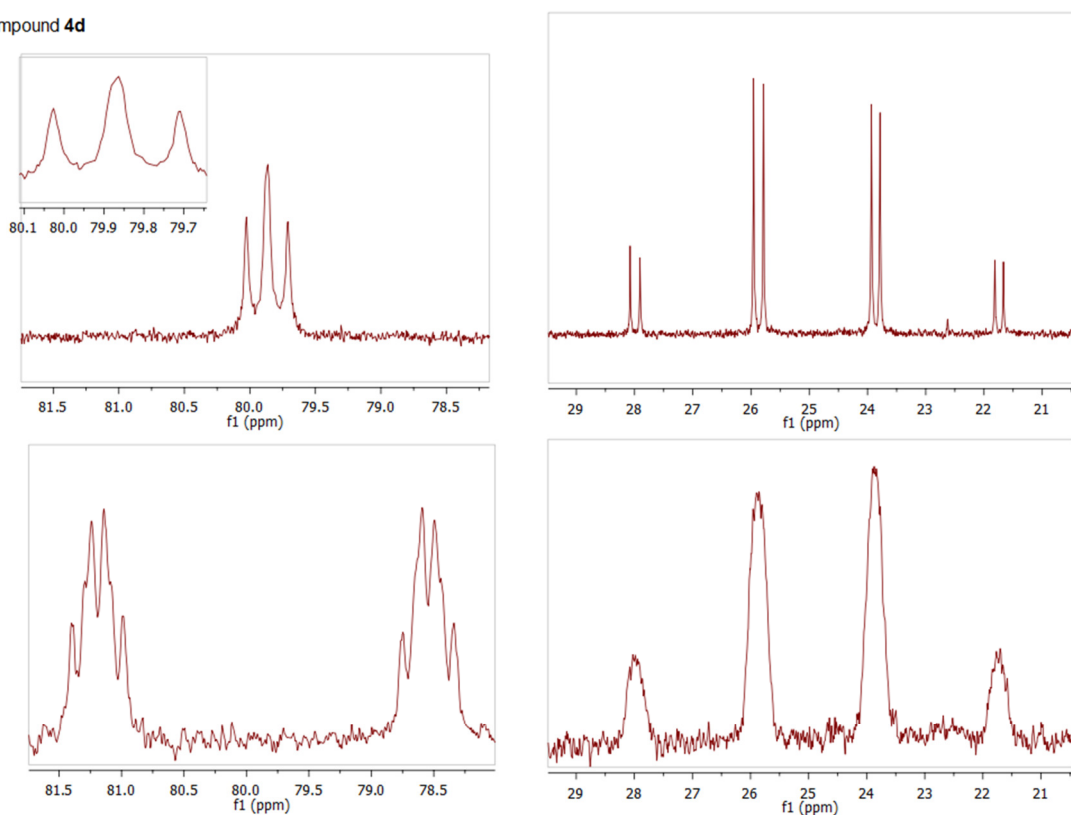


Figure S6. $^{31}\text{P}\{^1\text{H}\}$ (top) and ^{31}P (bottom) NMR signatures for $[\text{Ru}(\text{P}(\text{H})\text{ClCH}_2\text{SiMe}_2\text{C}_6\text{H}_4\text{CF}_3)\text{Cl}_2(\text{CO})(\text{PPh}_3)_2]$ (**4d**) plot on equivalent scales. The multiplicity of the chlorophosphane resonances is illustrated as inset for the proton decoupled spectrum.

Compound **4e**

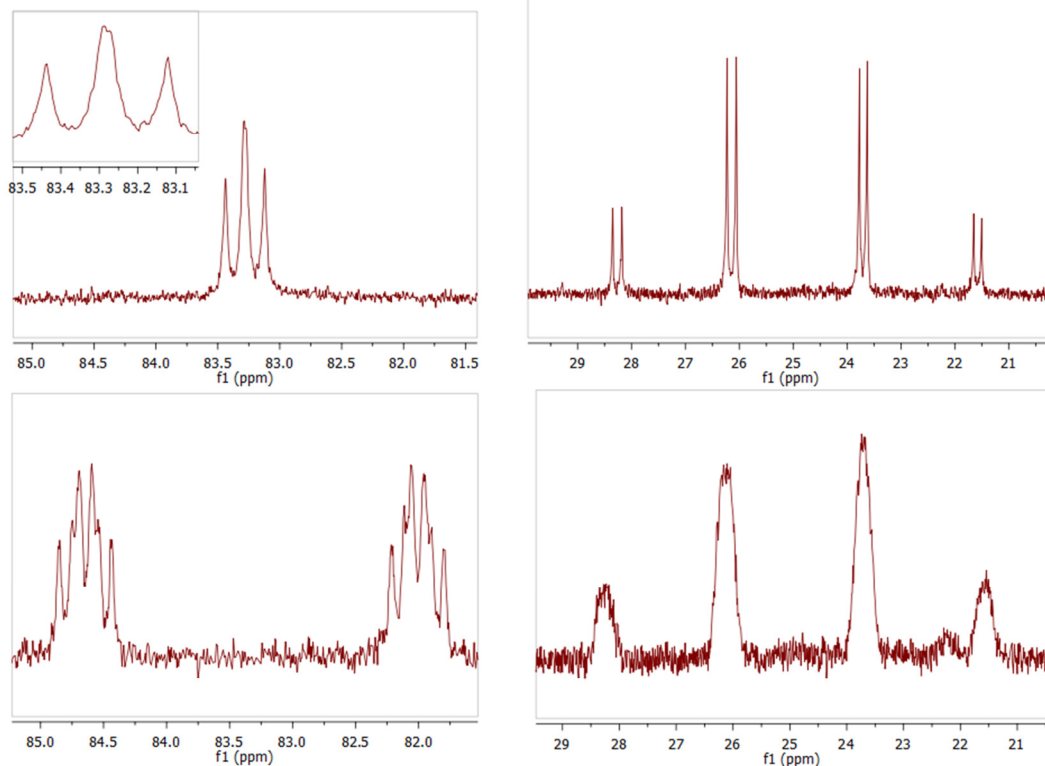
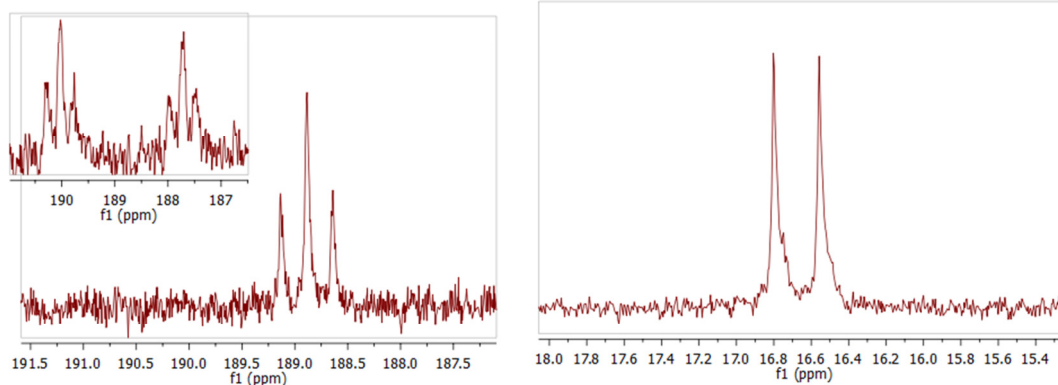


Figure S7. $^{31}\text{P}\{^1\text{H}\}$ (top) and ^{31}P (bottom) NMR signatures for $[\text{Ru}(\text{P}(\text{H})\text{ClCH}_2\text{SiMe}_2\text{n-Bu})\text{Cl}_2(\text{CO})(\text{PPh}_3)_2]$ (**4e**) plot on equivalent scales. The multiplicity of the chlorophosphane resonances is illustrated as inset for the proton decoupled spectrum.

Compound **3**



Compound **6**

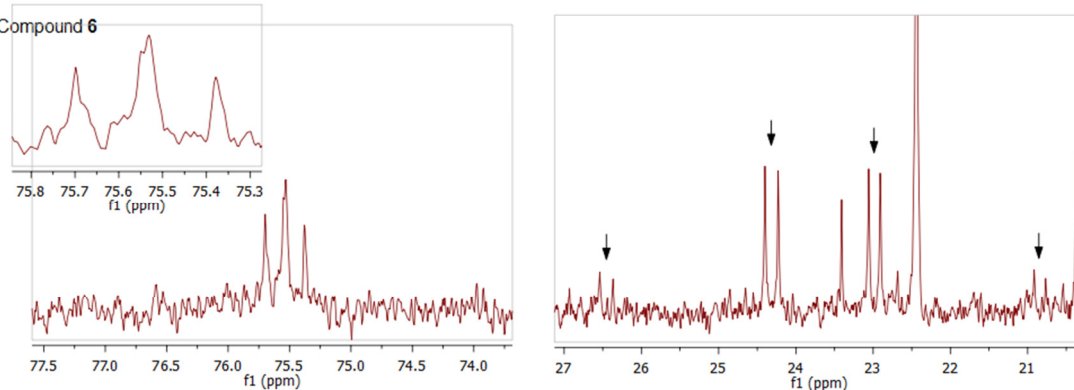


Figure S8. $^{31}\text{P}\{^1\text{H}\}$ NMR signatures for $[\text{Ru}(\text{P}(\text{H})=\text{CHtBu})\text{Cl}_2(\text{CO})(\text{PPh}_3)_2]$ (**3**) (top) with the proton coupled phosphacarbon resonance as inset, and $\text{Ru}(\text{P}(\text{H})\text{ClCH}_2\text{tBu})\text{Cl}_2(\text{CO})(\text{PPh}_3)_2$ (**6**) (bottom). The multiplicity (dd) of the chlorophosphane resonances is illustrated as inset for compound **6**.

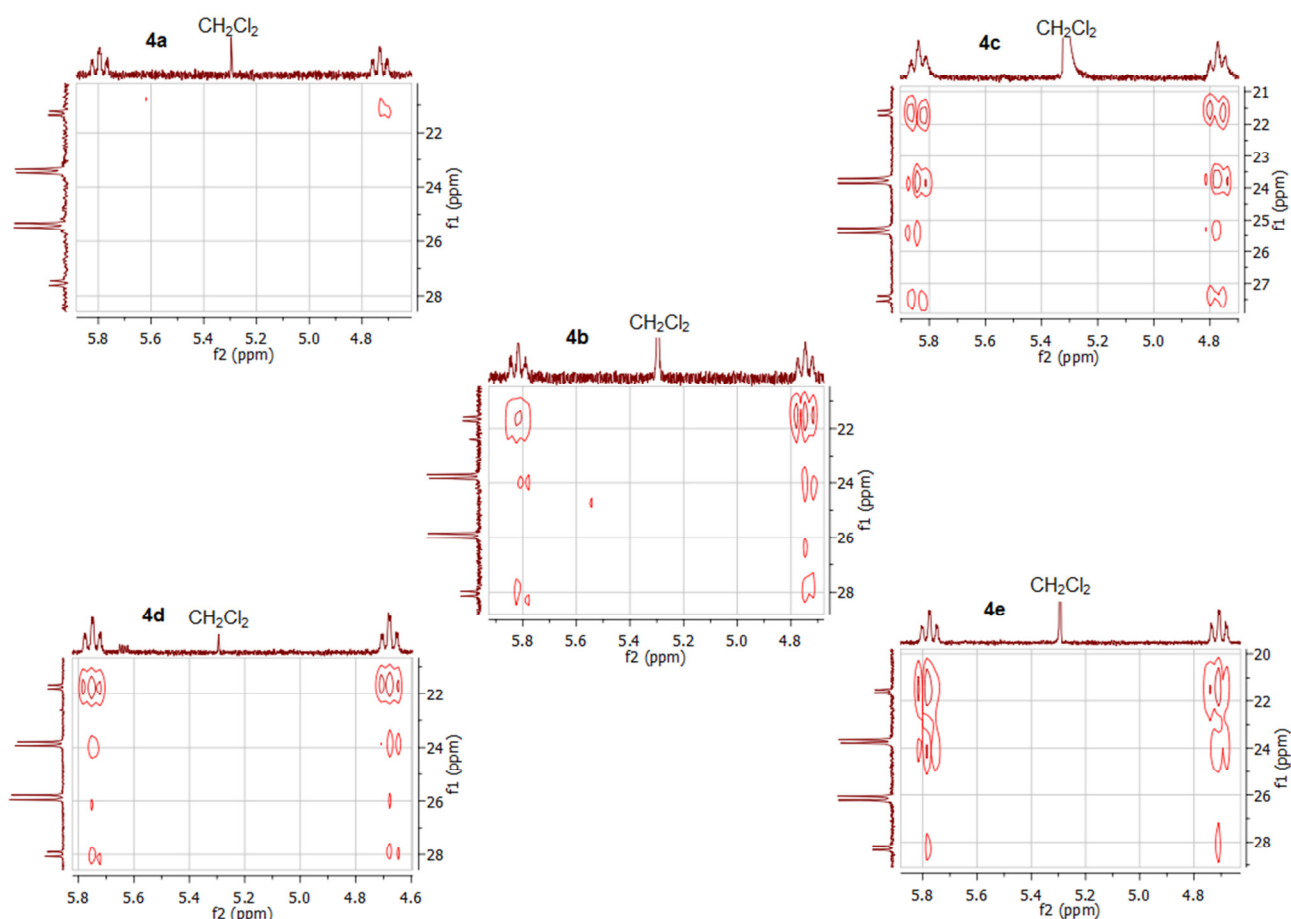


Figure S9: Expansions of the PPh₃ / PH region of ³¹P-¹H HMBC plots for compounds **4a-e**. The relative cross-peak integrals of correlations for the two separate PPh₃ units is in each case at least 5:1, indicative of a statistically significant difference in the magnitude of the H-P-Ru-P (³*J*) scalar interactions.

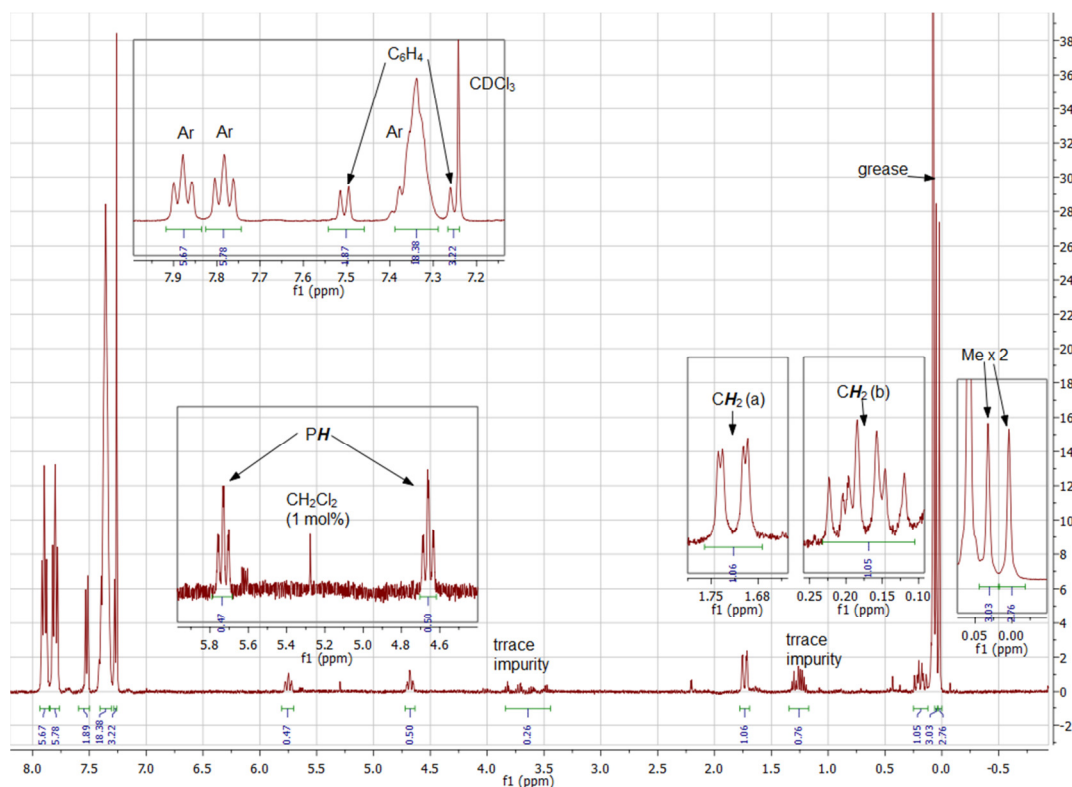


Figure S10a: ¹H-NMR spectrum of compound **4d** indicating trace impurities.

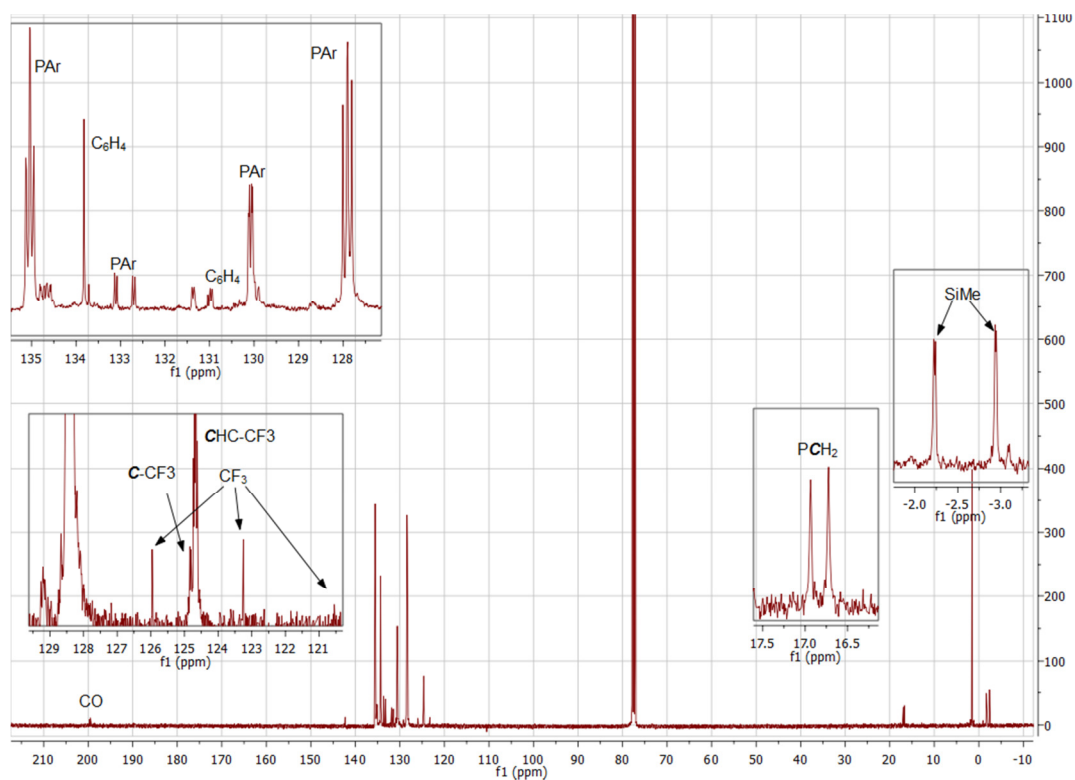


Figure S10b: $^{13}\text{C}\{^1\text{H}\}$ -NMR spectrum of compound **4d**.

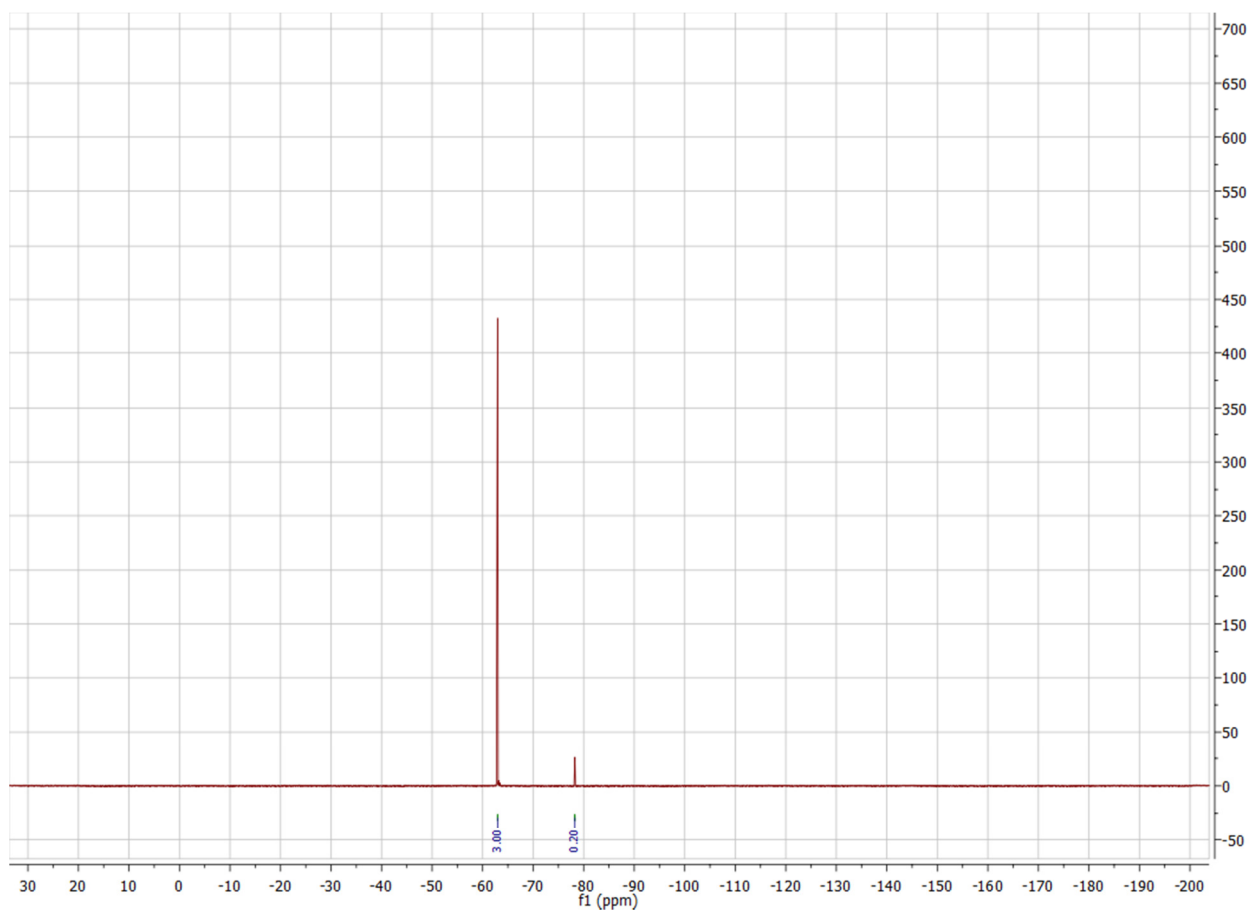


Figure S10c: ^{19}F -NMR spectrum of compound **4d**, indicating trace impurity.

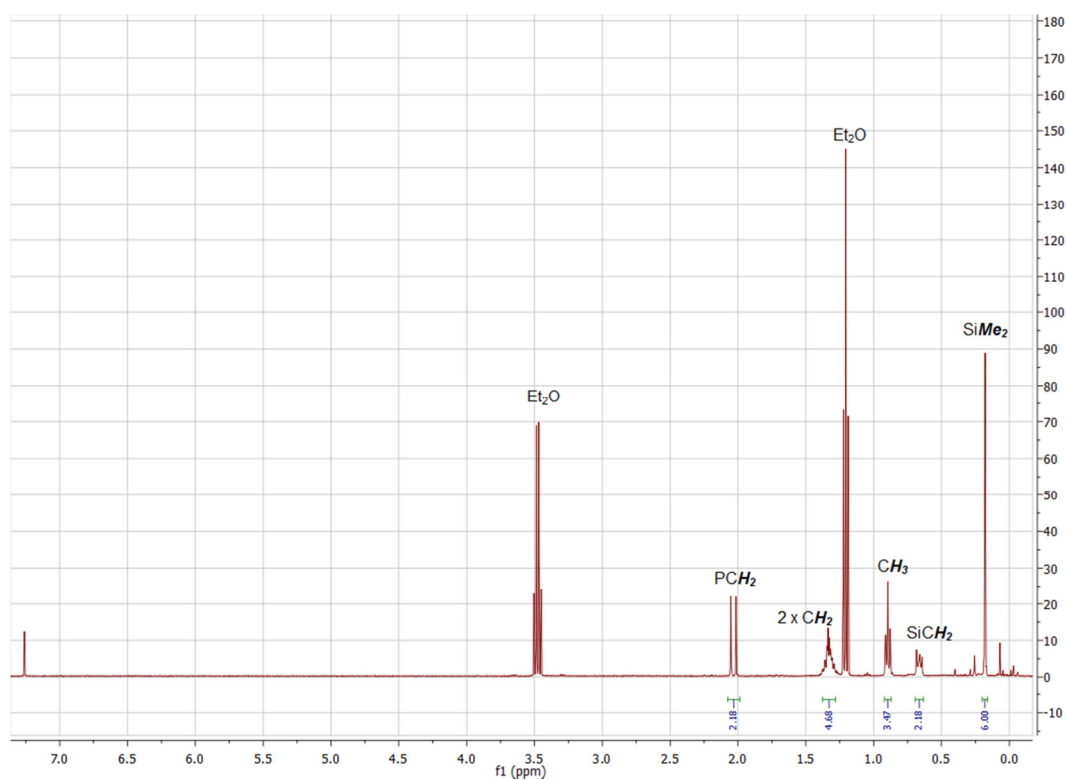


Figure S11a: ^1H -NMR spectrum of $\text{nBuMe}_2\text{SiCH}_2\text{PCl}_2$ indicating residual solvent.

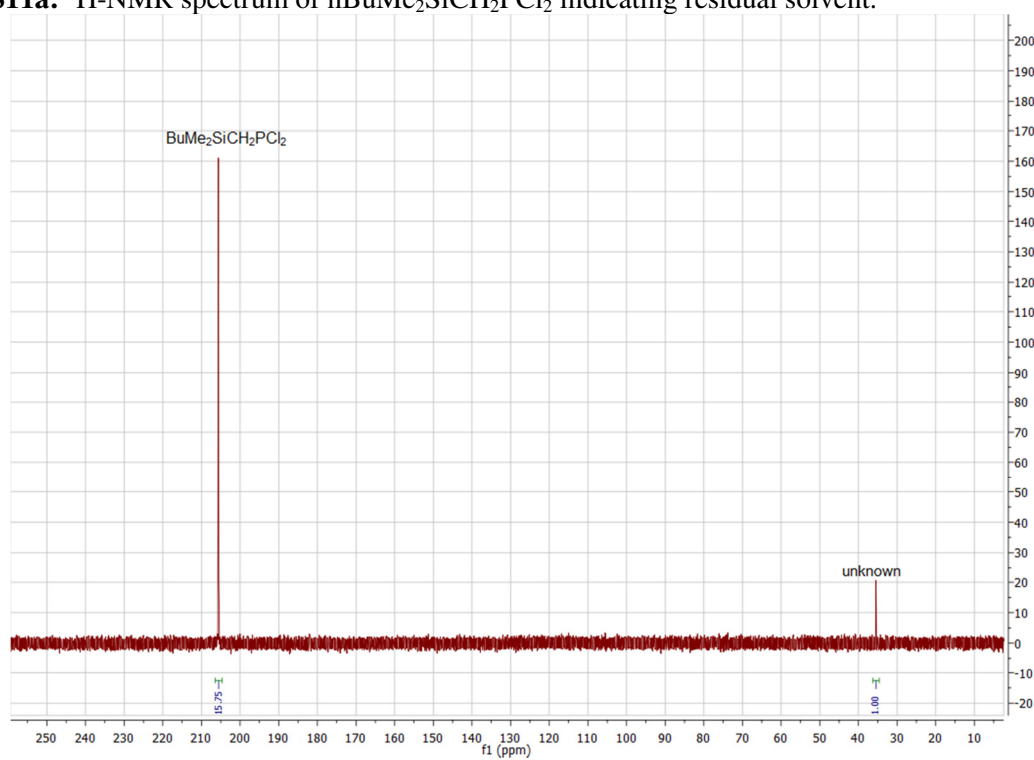


Figure S11b: ^{31}P -NMR spectrum of $\text{nBuMe}_2\text{SiCH}_2\text{PCl}_2$ indicating trace impurity.

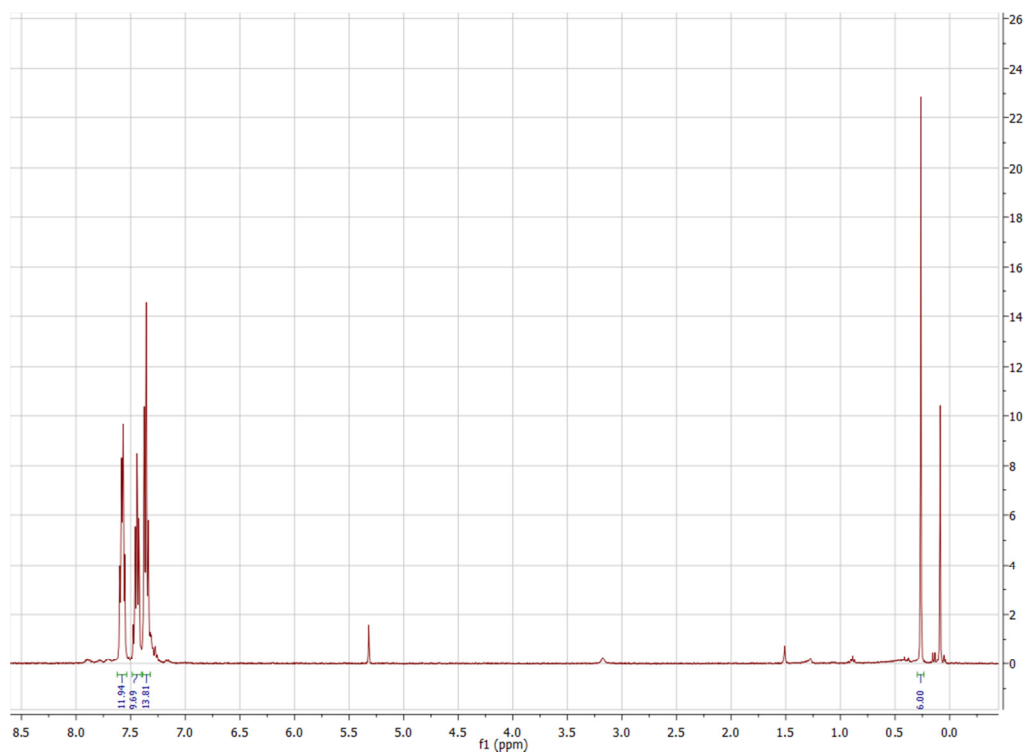


Figure S12a: ^1H -NMR spectrum of compound **2d**

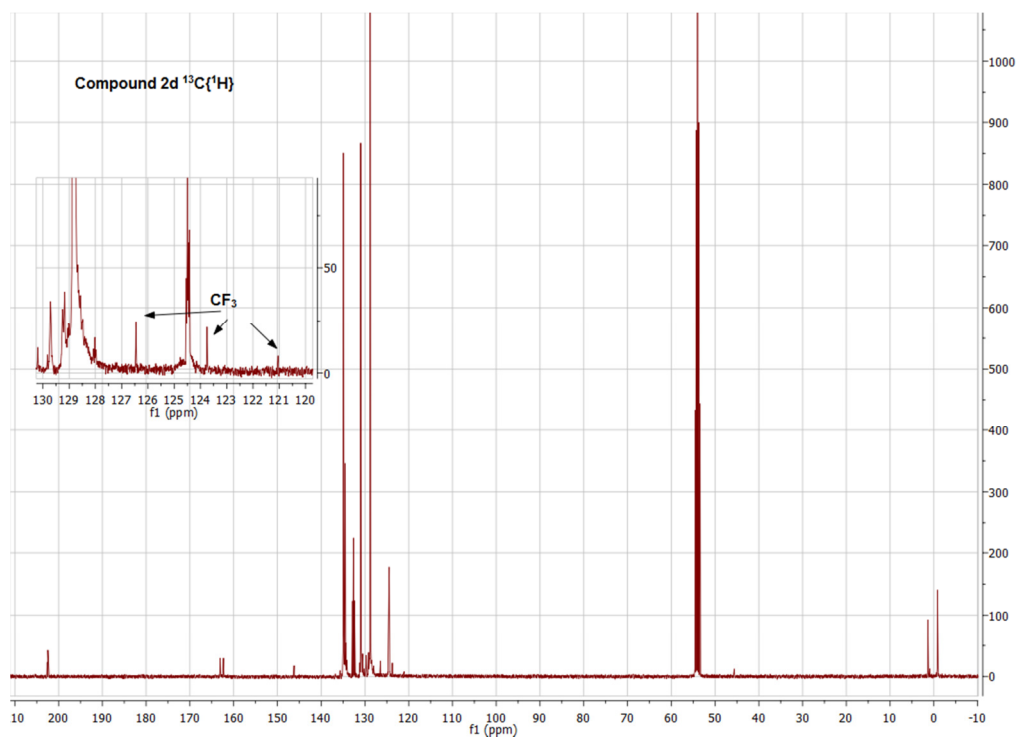


Figure S12b: $^{13}\text{C}\{^1\text{H}\}$ -NMR spectrum of compound **2d**.

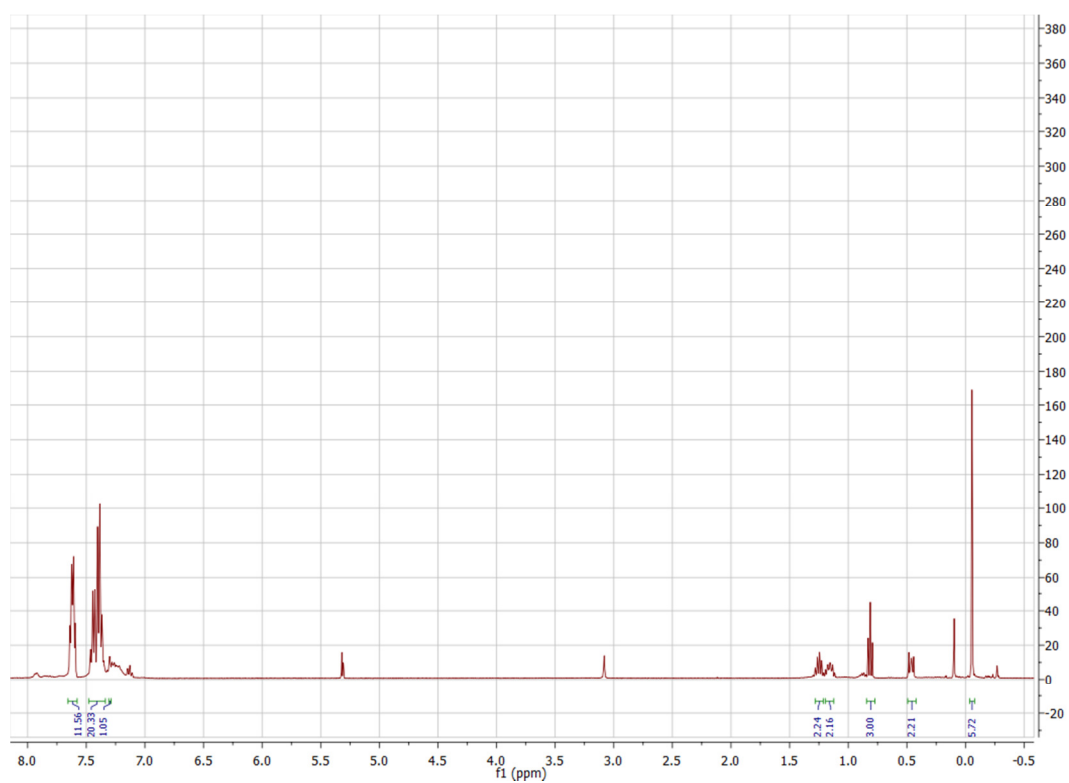


Figure S13a: ^1H -NMR spectrum of compound **2e**

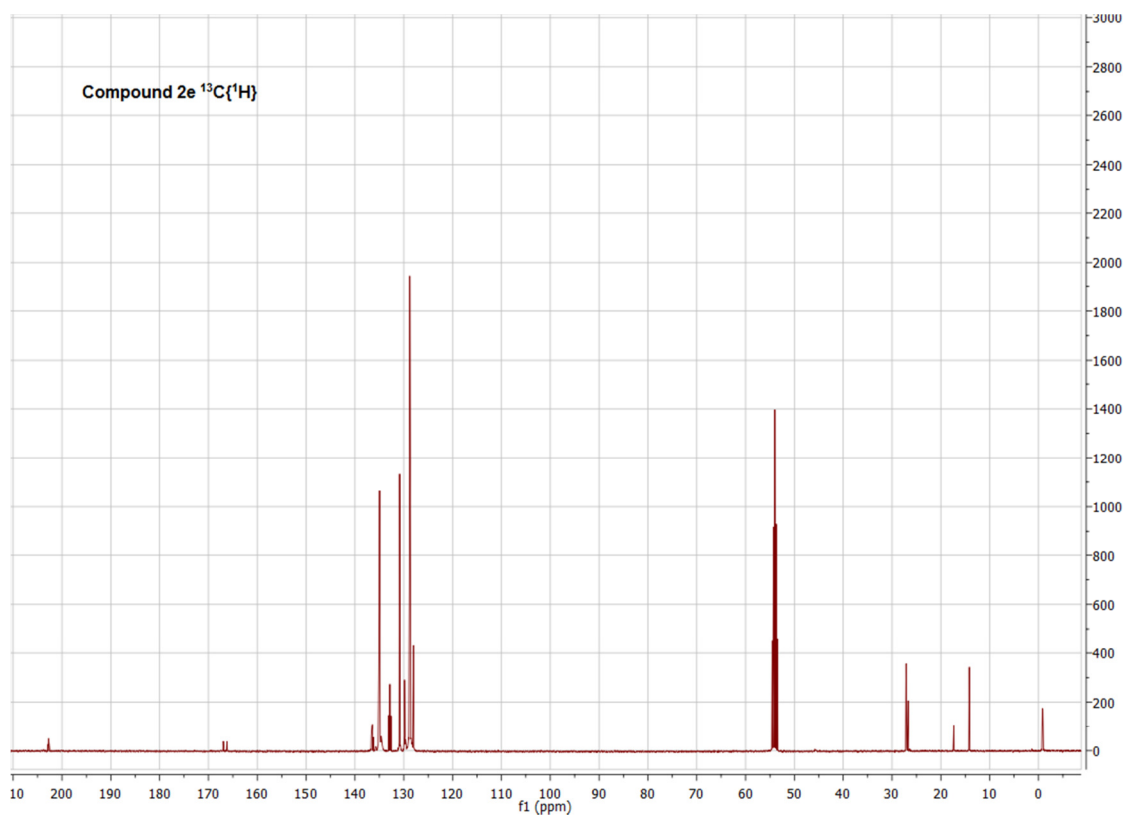


Figure S13b: $^{13}\text{C}\{^1\text{H}\}$ -NMR spectrum of compound **2e**.

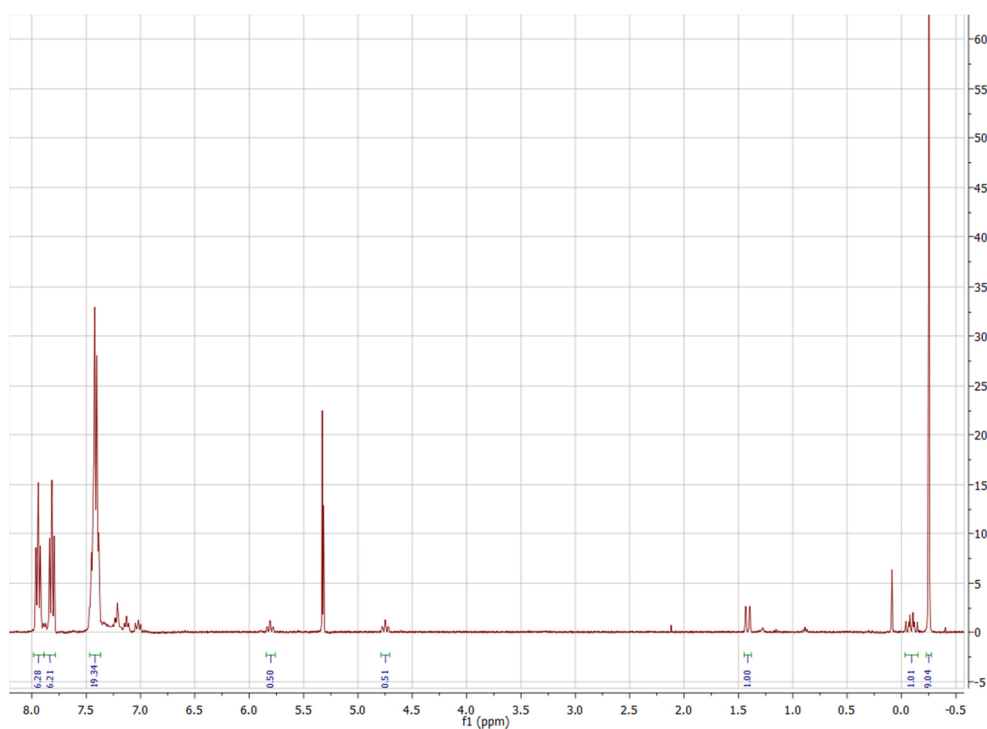


Figure S14a: ^1H -NMR (CD_2Cl_2) spectrum of compound **4a**

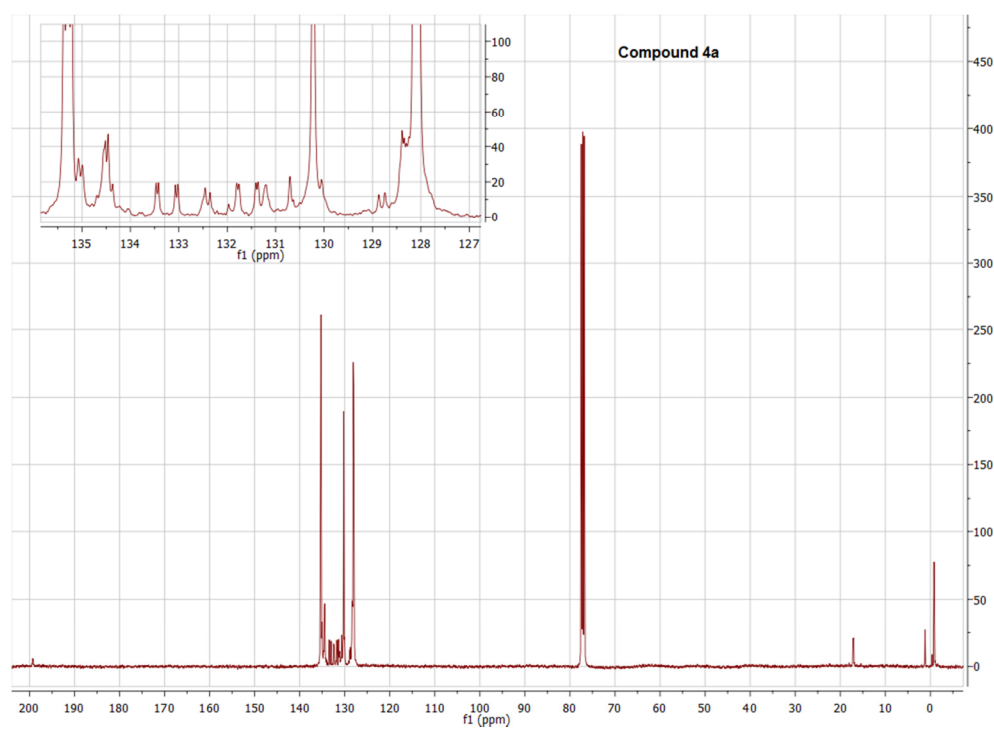


Figure S14b: $^{13}\text{C}\{^1\text{H}\}$ -NMR (CDCl_3) spectrum of compound **4a**.

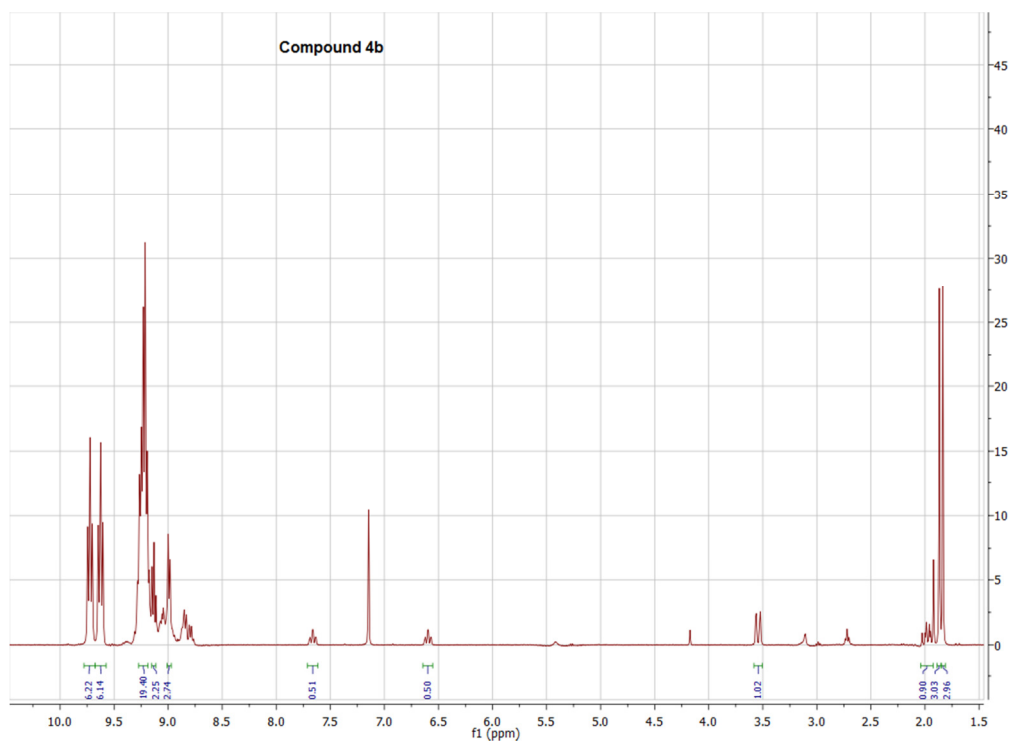


Figure S15a: ^1H -NMR (CD_2Cl_2) spectrum of compound **4b**

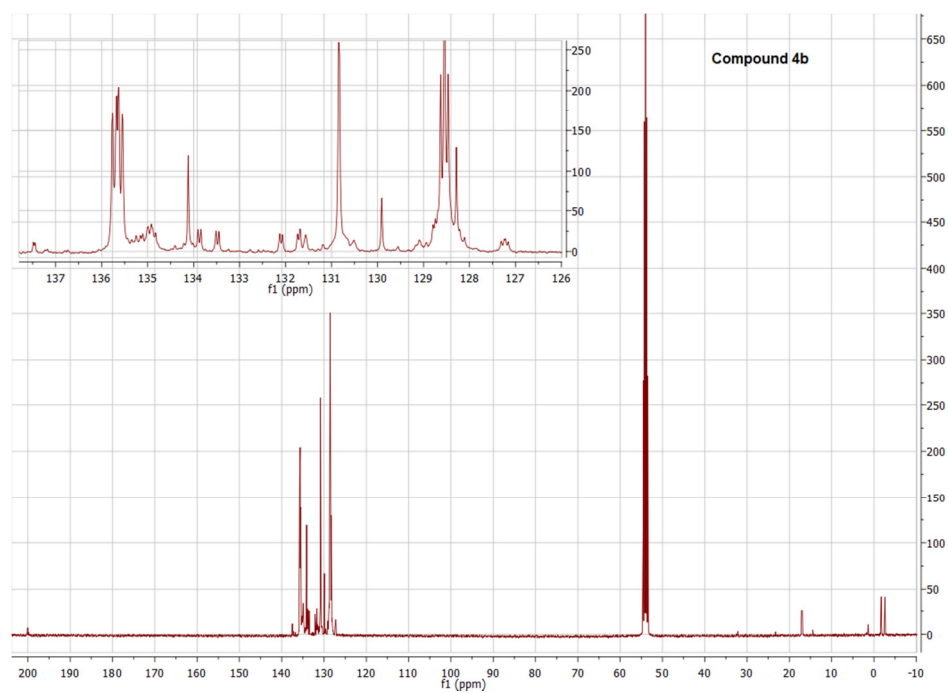


Figure S15b: $^{13}\text{C}\{^1\text{H}\}$ -NMR (CD_2Cl_2) spectrum of compound **4b**.

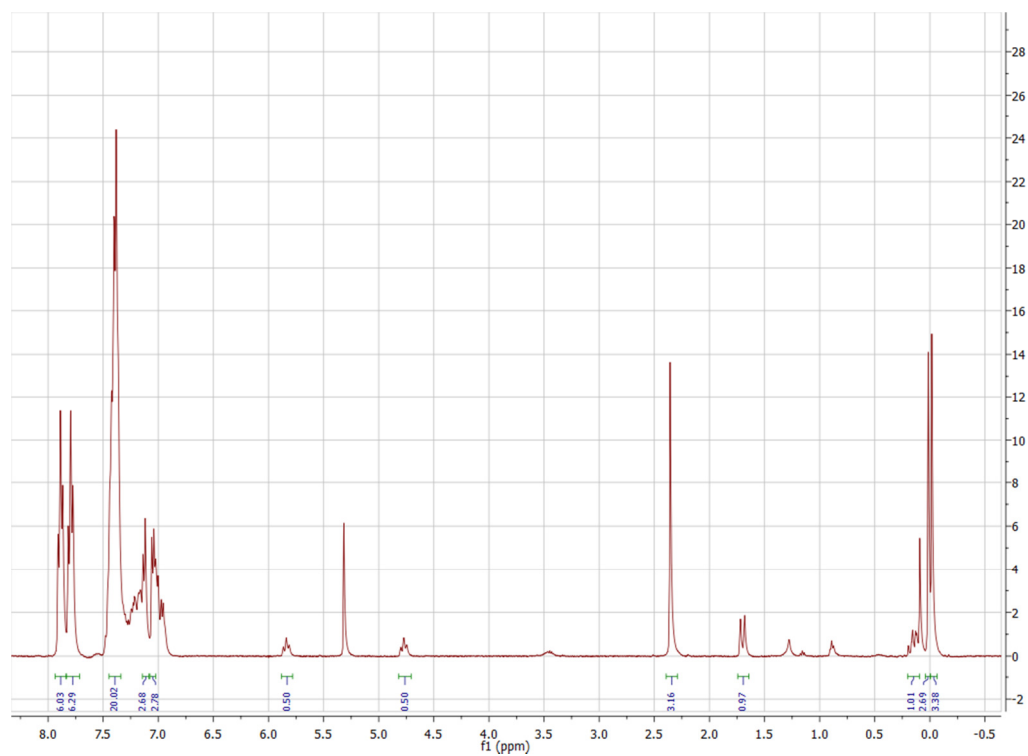


Figure S16a: ^1H -NMR (CD_2Cl_2) spectrum of compound **4c**

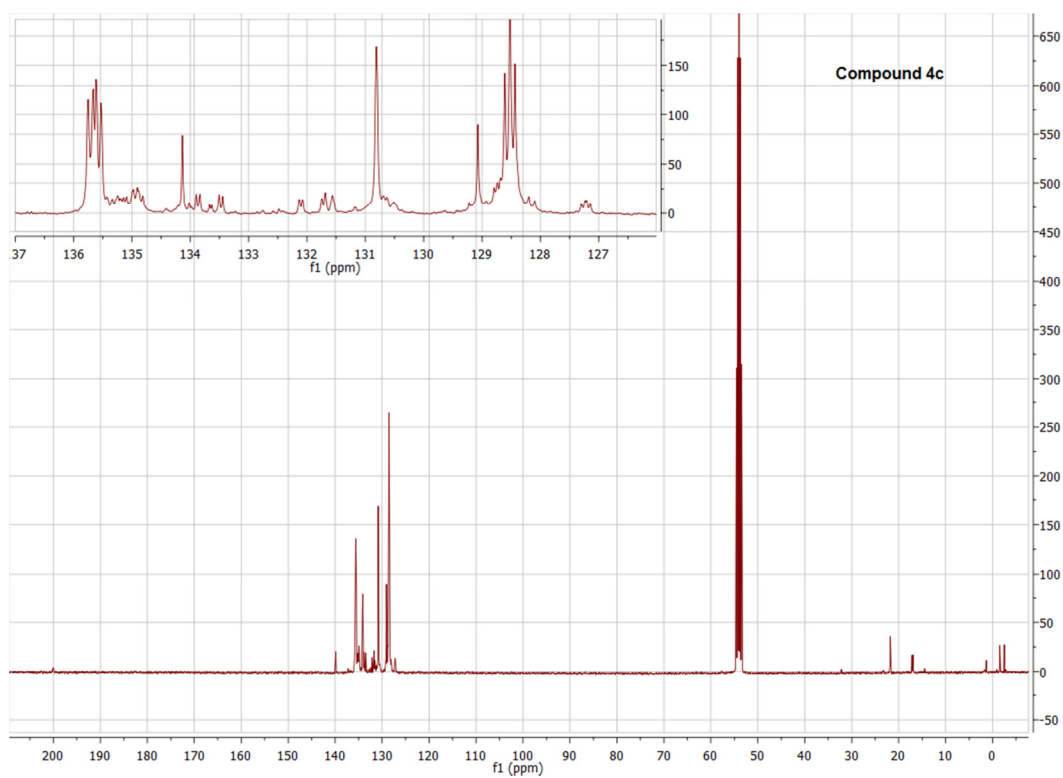


Figure S16b: $^{13}\text{C}\{^1\text{H}\}$ -NMR (CD_2Cl_2) spectrum of compound **4c**.

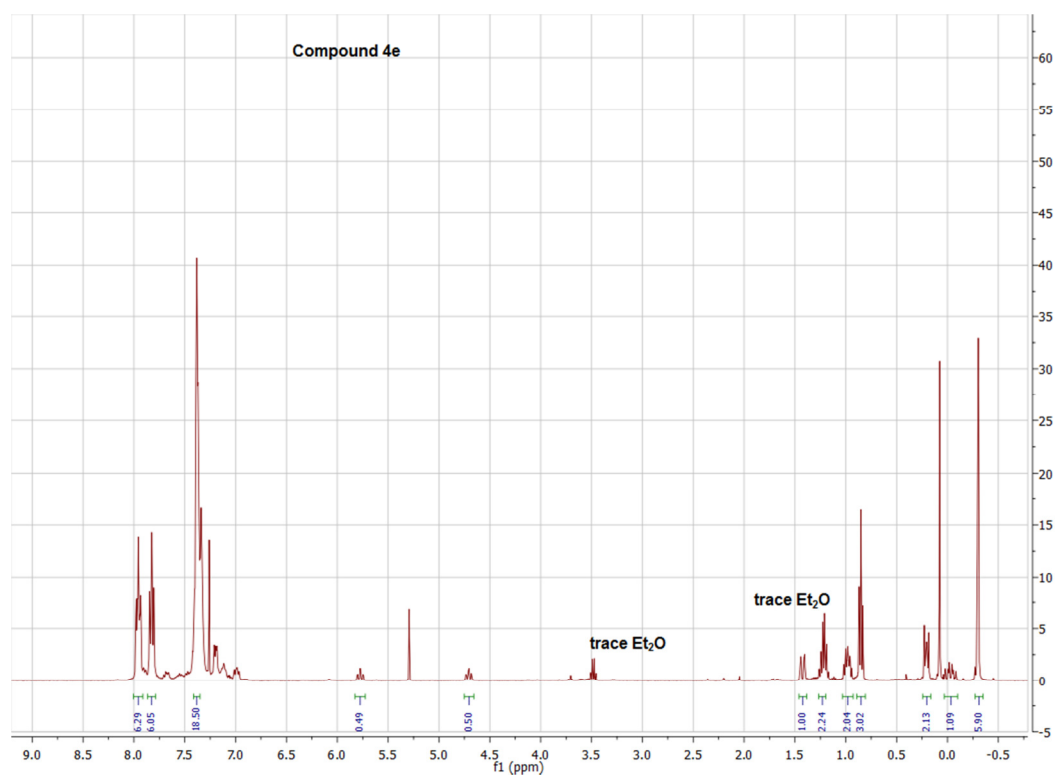


Figure S17a: ^1H -NMR (CD_2Cl_2) spectrum of compound **4e**

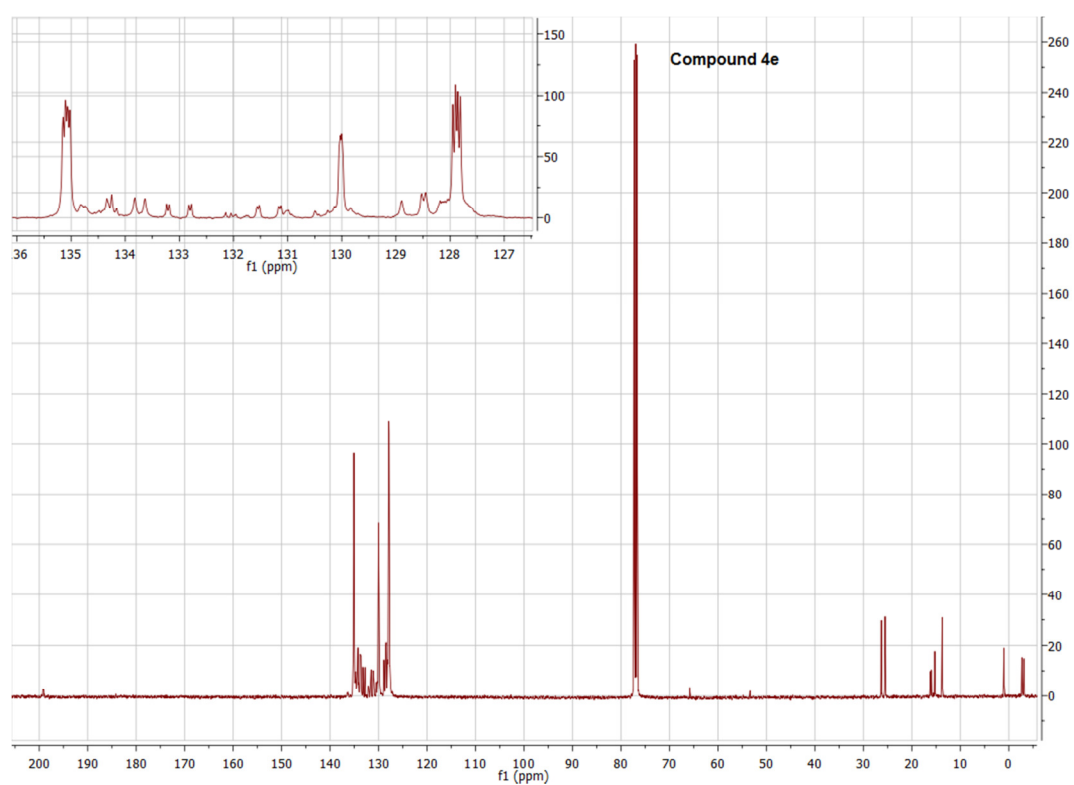


Figure S17b: $^{13}\text{C}\{^1\text{H}\}$ -NMR (CD_2Cl_2) spectrum of compound **4e**.